Non-Fermi-liquid and magnetic behaviour of the $Y_{1-x}U_xPd_3$ system



1996 J. Phys.: Condens. Matter 8 9793

(http://iopscience.iop.org/0953-8984/8/48/009)

J. Phys.: Condens. Matter **8** (1996) 9793–9806. Printed in the UK

# Non-Fermi-liquid and magnetic behaviour of the $Y_{1-x}U_xPd_3$ system

D A Gajewski, N R Dilley, R Chau and M B Maple

Physics Department and Institute for Pure and Applied Physical Sciences, University of California, San Diego, 9500 Gilman Drive, La Jolla, CA 92093-0319, USA

Received 17 September 1996

**Abstract.** The $Y_{1-x}U_xPd_3$ system exhibits an unconventional Kondo effect with non-Fermi-liquid characteristics at low temperatures for $x \lesssim 0.2$. Measurements of the low-temperature electrical resistivity and magnetization of high-purity samples with $0.05 \leqslant x \leqslant 0.15$ have been made as part of an effort to determine whether the non-Fermi-liquid behaviour persists to low U concentrations, i.e., whether it is a single-ion effect. Irreversible behaviour in the magnetization, reminiscent of spin glass freezing, is observed for samples with $0.25 \leqslant x \leqslant 0.55$, while long-range antiferromagnetic ordering has previously been established by neutron diffraction measurements for a sample with $x = 0.45$. Magnetic relaxation, ac magnetic susceptibility, and specific heat measurements were performed to investigate this unusual magnetic ordering.

## 1. Introduction

The $Y_{1-x}U_xPd_3$ system has received much attention in the literature recently because of its complex phase diagram and unusual low-temperature properties [1, 2]. For $x \leqslant 0.3$, the system exhibits the Kondo effect, where the electrical resistivity $\Delta\rho(T) \sim -\ln T$ and the magnetic susceptibility $\Delta\chi(t) \sim C/(T + \Theta)$ for temperatures $T$ much greater than the Kondo temperature $T_K$. The system also exhibits Fermi level tuning [3], in which the substitution of $U^{4+}$ for $Y^{3+}$ results in an increase in the Fermi energy $E_F$, and, in turn, an increase in the binding energy $\varepsilon_{5f} = |E_F - E_{5f}|$ of the localized uranium 5f electrons. This leads to an exponential dependence of $T_K$ on the uranium concentration $x$, as can be seen from the expression for $T_K$:

$$T_K \sim T_F \exp\Big(-\varepsilon_{5f}/\langle V_{kf}^2\rangle N\big(E_F\big)\Big) \tag{1}$$

where $\langle V_{kf}^2\rangle$ is the hybridization matrix element between the conduction band and the localized U 5f states, and $N(E_F)$ is the density of states at the Fermi level. For $T < T_K$, the system exhibits unusual temperature dependences of its transport, thermodynamic, and magnetic properties. In particular, for $Y_{0.8}U_{0.2}Pd_3$, the most thoroughly studied composition in the series, $\Delta\rho(T)/\Delta\rho(0) \sim 1 - a(T/T_K)$, the specific heat coefficient $\Delta C_p(T)/T \sim -(1/bT_K)\ln T$, and $\Delta\chi(T)/\Delta\chi(0) \sim 1 - c(T/T_K)^{1/2}$ ($a$, $b$, and $c$ are constants of order unity), over at least two decades of temperature. Since these temperature dependences have also been observed in several other uranium- and cerium-based materials, a new class of f-electron materials whose physical properties exhibit non-Fermi-liquid behaviour at low temperature has been identified, of which $Y_{1-x}U_xPd_3$ is the first example [4]. These temperature dependences are to be compared to those of a conventional

0953-8984/96/489793+14$19.50  

Kondo system which behaves as a local Fermi liquid: $\Delta\rho(T)/\Delta\rho(0) \sim 1 - (T/T_K)^2$, $\Delta C_p(T)/T \sim \gamma$, and $\Delta\chi(T) \sim \Delta\chi(0)$, for $T \ll T_K$.

Several different microscopic models have been considered in an attempt to explain the non-Fermi-liquid behaviour in $Y_{1-x}U_xPd_3$. In 1991, Seaman *et al* [1] compared their results to the quadrupolar Kondo model in which the scattering of conduction electrons in two channels by the electric quadrupole moment of the uranium ions produces non-Fermi-liquid behaviour at low temperature. This explanation requires that the ground state of the $U^{4+}$ ions in the cubic crystalline electric field (CEF) be the nonmagnetic $\Gamma_3$ doublet which carries a quadrupole moment. Inelastic neutron scattering measurements by Mook *et al* on $Y_{0.8}U_{0.2}Pd_3$ revealed only weak quasi-elastic scattering with a linewidth of less than 0.2 meV [5]. Since this value is much less than the Kondo energy scale for this system, they concluded that the ground state of the uranium ions was the nonmagnetic $\Gamma_3$. However, more recent neutron scattering experiments by Dai *et al* [6] using a polarized neutron source indicate that the ground state of $U^{4+}$ in $Y_{0.55}U_{0.45}Pd_3$, and possibly also $Y_{0.8}U_{0.2}Pd_3$, is actually the magnetic $\Gamma_5$ triplet. This would exclude the possibility of an electric quadrupolar Kondo effect, unless the $\Gamma_5$ is split at low temperatures due, for example, to a local change in crystal symmetry from cubic to tetragonal or hexagonal [7], or to a crossover to a $\Gamma_3$ ground state at $x = 0.2$. McCarten *et al* concluded from thermopower measurements on $Y_{1-x}U_xPd_3$ that there is some sort of crossover or transition in electronic structure near $x = 0.2$ [8]. Aoki *et al* have concluded that $Y_{1-x}U_xPd_3$ behaves like an ordinary Fermi liquid for $x < 0.1$, based on resistivity, magnetization, and specific heat measurements [9].

Andraka and Tsvelik observed similar non-Fermi-liquid behaviour in $Y_{0.8}U_{0.2}Pd_3$, but found that the transport properties obey different scaling relations than the thermodynamic properties [2]. They argued that the data are inconsistent with a single-impurity interpretation, and suggested that the non-Fermi-liquid behaviour is caused by fluctuations of an order parameter above a second-order phase transition at zero temperature. Dai *et al* found no magnetic ordering in $Y_{0.8}U_{0.2}Pd_3$ above 0.2 K, but observed critical fluctuations associated with antiferromagnetic ordering on cooling from 77 to 0.2 K with the same wavevector as that seen in the sample with $x = 0.45$ [6]. In addition, the $T_{irr}$ versus $x$ curve (see figure 1) extrapolates to $T = 0$ near $x = 0.2$. Notably, von Löhneysen *et al* have obtained compelling evidence that the non-Fermi-liquid behaviour in the $CeCu_{6-x}Au_x$ system is driven by an antiferromagnetic phase transition near $T = 0$ K [10].

In order to investigate the microscopic physics underlying the non-Fermi-liquid behaviour in the $Y_{1-x}U_xPd_3$ system, we have fabricated high-purity samples with $x = 0.15$, 0.10, and 0.05 in an attempt to approach the single-impurity limit. We present measurements of the electrical resistivity $\Delta\rho(T)$ and magnetic susceptibility $\Delta\chi(T)$ to low temperatures in order to investigate the persistence of the non-Fermi-liquid behaviour for uranium concentrations less than 0.2.

In order to assess the applicability of the model of a second-order phase transition at $T = 0$ to explain the non-Fermi-liquid behaviour, it is important to understand the nature of the magnetic ordering that is observed for uranium concentrations $x \gtrsim 0.2$. For $0.25 \leqslant x \leqslant 0.55$, the magnetization of $Y_{1-x}U_xPd_3$ exhibits hysteresis reminiscent of spin glass behaviour [11] below an ordering temperature $T_{irr}$; this temperature generally increases with increasing $x$. For $x < 0.25$, no hysteresis has been observed. Lopez de la Torre has performed magnetic relaxation and nonlinear susceptibility measurements for $x = 0.4$ to characterize the spin glass state [12]. Muon spin relaxation measurements on a sample with $x = 0.4$ are consistent with spin glass freezing [13], while neutron diffraction experiments showed that a sample with $x = 0.45$ exhibits long-range antiferromagnetic ordering [6].

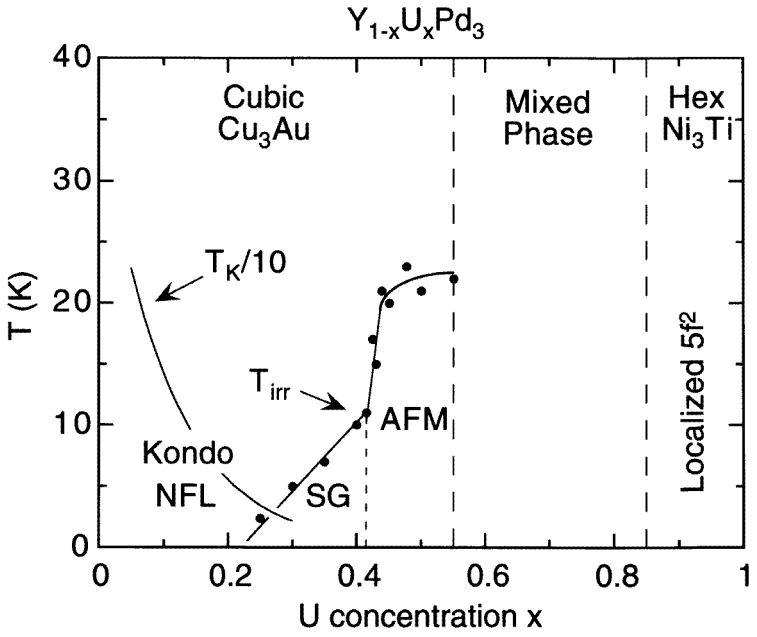


**Figure 1.** The temperature $T$–U concentration $x$ phase diagram of the $Y_{1-x}U_xPd_3$ system. NFL, non-Fermi-liquid; SG, spin glass; AFM, antiferromagnetism.

These seemingly contradictory results indicate that the magnetic ordering regime of the phase diagram of $Y_{1-x}U_xPd_3$ is in need of further study. We have thus performed dc and ac magnetization, magnetic relaxation, electrical resistivity, and specific heat measurements on several $Y_{1-x}U_xPd_3$ samples with $0.25 \leqslant x \leqslant 0.55$ to more thoroughly characterize the nature of the magnetic ordering.

## 2. Experimental details

Polycrystalline samples of $Y_{1-x}U_xPd_3$ were prepared by arc melting stoichiometric amounts of the elemental metals under an ultra-high-purity argon atmosphere. Samples with $x < 0.2$ were made using high-purity electropolished yttrium metal (99.99%) from Ames National Laboratory, palladium (99.99%) from Engelhard, and uranium (99.977%) from New Brunswick Laboratories. Samples with $x > 0.2$ were made using the same uranium, but with 99.9% pure yttrium and 99.97% pure palladium. Electrical resistivity $\rho(T)$ measurements were performed using a four-wire, low-frequency ac technique (16 Hz) from 1.2 to 300 K in a $^4$He cryostat. ac (10, 100, 1000 Hz) and dc magnetization measurements were made in a commercial SQUID magnetometer from 1.8 to 300 K, and dc magnetization was measured using a Faraday magnetometer from 0.4 to 10 K in a $^3$He refrigerator. Specific heat $C_p(T)$ was measured using a semi-adiabatic heat pulse calorimeter with a $^3$He refrigeration stage from 0.5 to 30 K.

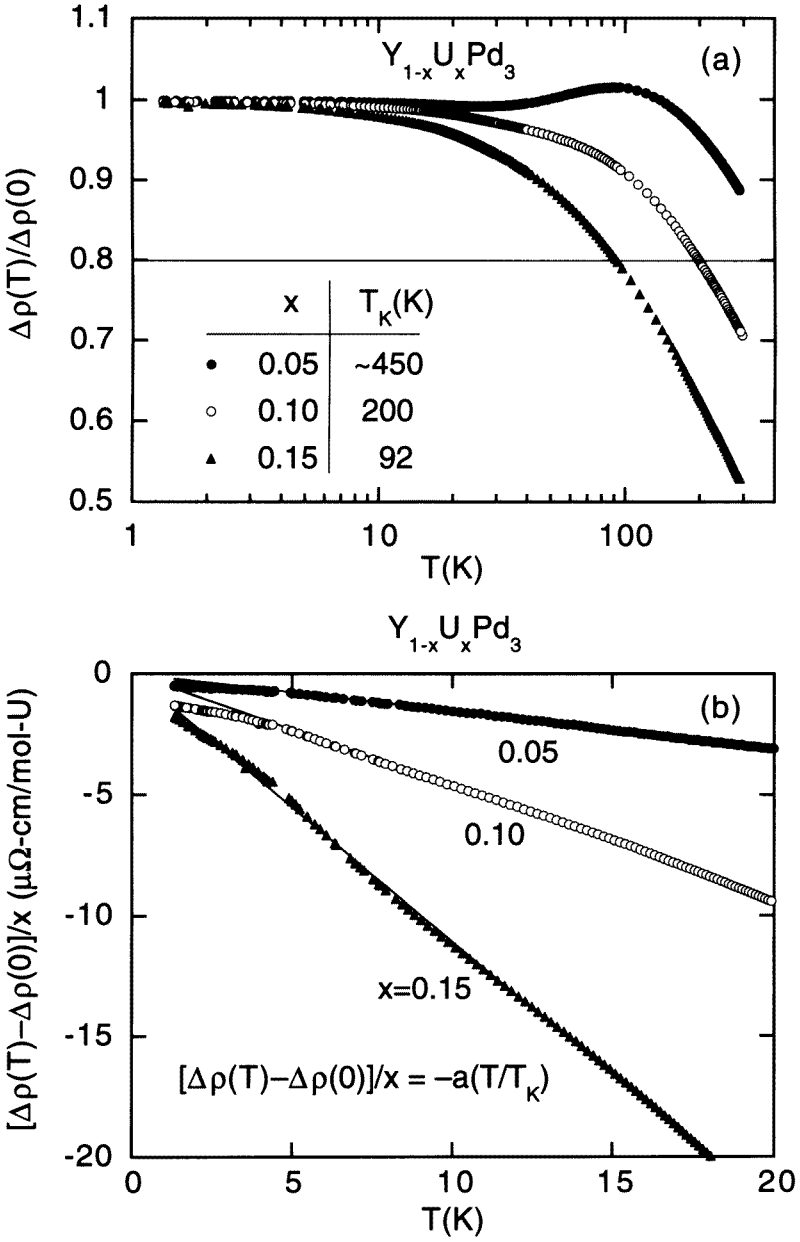


**Figure 2.** (a) The uranium contribution to the electrical resistivity $\Delta\rho(T)$ of $Y_{1-x}U_xPd_3$, normalized to its linearly extrapolated zero-temperature value $\Delta\rho(0)$, versus log $T$. The Kondo temperature $T_K$ is defined using the criterion $\Delta\rho(T_K)/\Delta\rho(0) \equiv 0.8$. (b) Electrical resistivity $\Delta\rho(T)$ minus $\Delta\rho(0)$, normalized by the uranium concentration $x$, versus temperature $T$, and linear fits from 5 to 20 K.

## 3. Results

### *3.1. The Kondo regime*

The $Y_{1-x}U_xPd_3$ system exhibits the Kondo effect, as can be seen from the logarithmic temperature dependence of the uranium contribution to the electrical resistivity, $\Delta\rho(T)$, in

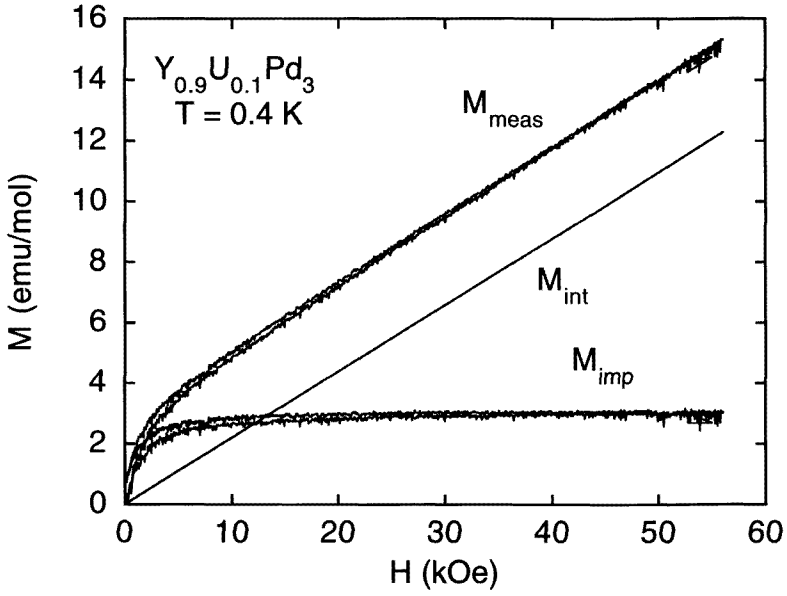


**Figure 3.** Magnetization $M$ versus applied field $H$ of a high-purity sample of $Y_{0.9}U_{0.1}Pd_3$ at 0.4 K, measured in a Faraday magnetometer. The measured moment $M_{meas} = M_{int} + M_{imp}$. (See the text for a discussion.)

figure 2(a). The resistivity of a sample of high-purity $YPd_3$ has been subtracted from $\rho(T)$ to obtain $\Delta\rho(T)$, and the data have been normalized by the zero-temperature value and by the uranium concentration. The Kondo temperature $T_K$ is defined as the temperature at which $\Delta\rho(T)$ reaches 80% of its zero-temperature value, and is tabulated in the figure. It is evident that $T_K$ decreases rapidly with increasing $x$, which is consistent with Fermi level tuning. Possible sources of the maximum in $\Delta\rho(T)$ for the sample with $x = 0.05$ include the depopulation of a uranium crystal field level, or, possibly, errors in the subtraction of the resistivity of the host compound (e.g., breakdown of Matthieson's rule, uncertainty in geometrical factor, etc). Experiments at lower uranium concentrations may help to resolve this issue.

We observe a roughly linear temperature dependence of $\Delta\rho(T)$ for $x = 0.05$, 0.1, and 0.15 between $\sim$1 and 20 K. This is shown in figure 2(b) where $[\Delta\rho(T) - \Delta\rho(0)]/x$ is plotted versus temperature. The zero-temperature value $\Delta\rho(0)$ was determined by fitting $\Delta\rho(T)$ to a straight line using a least-squares fitting routine from 5 to 20 K, and defining the $y$-intercept as $\Delta\rho(0)$. These data are also consistent with Fermi level tuning, as can be seen from the expression

$$\Delta\rho(T) - \Delta\rho(0) = -a\big(T/T_K\big). \tag{2}$$

There seems to be some deviation from this linear behaviour for the samples with $x = 0.1$ and 0.05 below $\sim$3 K, which could represent a power law temperature dependence slightly greater than 1.0, or, possibly, a recovery of Fermi liquid behaviour at lower temperature. Measurements at lower temperatures are reported in another article in this volume [14].

Shown in figure 3 is the measured magnetization at 0.4 K for $Y_{0.9}U_{0.1}Pd_3$. For Kondo systems, one expects the intrinsic magnetization to be linear in the applied field provided that $\mu_B H \ll k_B T_K$, which is the case here. Therefore, we interpret the measured magnetization

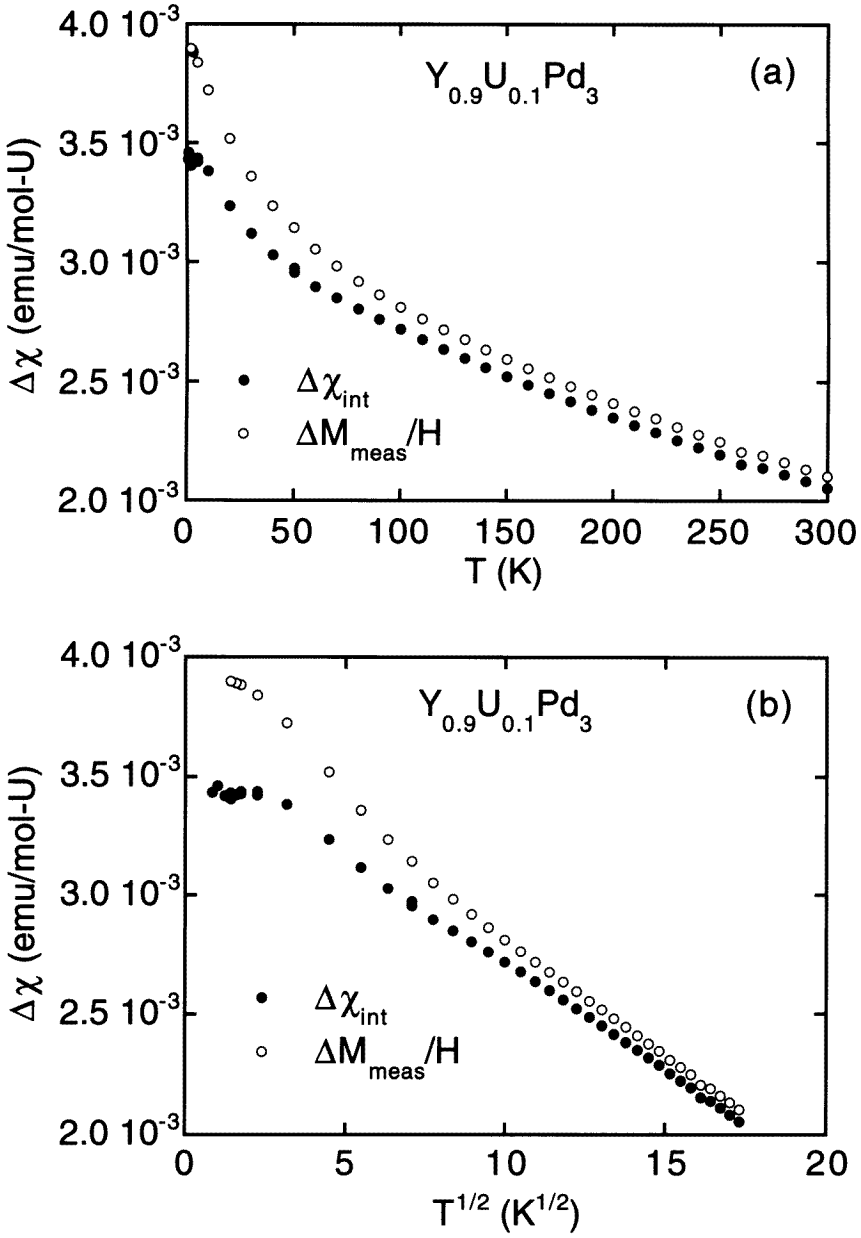


**Figure 4.** (a) The intrinsic magnetic susceptibility $\Delta\chi_{int}(T)$ of $Y_{0.9}U_{0.1}Pd_3$, and measured magnetization divided by the applied field, $\Delta M_{meas}/H$, versus temperature $T$. The susceptibility of $YPd_3$, assumed diamagnetic and constant in temperature, has been subtracted. (b) $\Delta\chi_{int}$ and $\Delta M_{meas}/H$ data versus $T^{1/2}$.

as the superposition of an intrinsic contribution associated with the uranium ions ($M_{int}$) and an extrinsic term ($M_{imp}$) which is due to magnetic impurities other than randomly substituted uranium ions. These magnetic impurities could be rare earths, 3d transition metals, or even uranium, in the form of clusters or located in the interstices. At the lowest temperatures and

the highest fields, the impurity moments are mostly saturated, so that one can estimate the intrinsic susceptibility as the slope of the magnetization curve at high fields. Subtracting a straight line passing through the origin with this slope yields the impurity magnetization as a function of field. The impurity contribution, $M_{imp}$, was assumed not to take an explicit functional form, but to scale as $H/(T+\theta)$, where $\theta$ is a small Curie–Weiss temperature due to the interaction of the impurity moments with one another. The impurity magnetization was then scaled with $H/(T+\theta)$ and subtracted from the $M$ versus $H$ isotherms at higher temperatures. Finally, the remaining data were fitted to a straight line using a least-squares fitting routine to obtain the final intrinsic susceptibility $\chi_{int}$. This general method was used previously to analyse magnetization data for $Y_{0.8}U_{0.2}Pd_3$ in [4], where $M_{int}$ was represented by a Brillouin function of $H/(T+\theta)$, and in [15], where $M_{int}$ was also assumed to take no particular functional form but to scale with $H/(T+\theta)$. The susceptibility of $YPd_3$, which was taken from the work of Gardner *et al* [16] and set equal to a constant value of $-1.8$ $\mu$emu g$^{-1}$, was subtracted from the data to obtain $\Delta\chi_{int}$.

The results for the intrinsic susceptibility are presented in figure 4(a). Clearly, the impurity contribution is significant, even up to 100 K. In figure 4(b), the plot of the intrinsic susceptibility versus $T^{1/2}$ shows that $\Delta\chi_{int}$ exhibits square root behaviour over a large temperature range. Below approximately 5 K, $\Delta\chi_{int}$ deviates from this $T^{1/2}$ behaviour and appears to saturate to a constant value. This crossover temperature corresponds roughly to the temperature at which the resistivity starts to deviate from linear behaviour. Therefore, we speculate that these features could signal a crossover to Fermi liquid behaviour at low temperatures. In contrast, the non-Fermi-liquid behaviour for the $x = 0.15$ and 0.2 compounds seems to persist into the millikelvin temperature range. Experiments at lower temperatures and lower uranium concentrations will be conducted to clarify this situation.

### *3.2. The magnetic ordering regime*

The magnetic susceptibility of $Y_{1-x}U_xPd_3$ is hysteretic under zero-field cooling (ZFC) and field cooling (FC), with irreversibility temperatures $T_{irr}$ that generally increase with $x$ (see figure 5). For $0.25 \leqslant x \leqslant 0.415$, $T_{irr}$ increases approximately linearly with $x$, then increases sharply near $x = 0.42$, and finally bends over and levels off in the range $0.45 \leqslant x \leqslant 0.55$. $\mu$SR measurements found spin-glass-like magnetic order in a sample with $x = 0.4$ [13] with a spin glass freezing temperature $T_g = 12$ K that approximately coincides with $T_{irr}$ for that sample. However, neutron scattering revealed the onset of long-range antiferromagnetic ordering in a sample with $x = 0.45$ below a Néel temperature $T_N = 21$ K [6], which also agrees with $T_{irr}$. We have therefore postulated that the sharp upturn in the $T_{irr}$ versus $x$ curve marks the boundary between short-range spin glass freezing and long-range antiferromagnetic ordering, and we have performed several experiments to test this hypothesis.

Magnetic susceptibility $\chi_{ac}$ versus temperature data, taken at 10, 100, and 1000 Hz, are presented in figure 6 for (a) $x = 0.4$ and (b) $x = 0.45$. For the sample with $x = 0.4$, there is a peak in the in-phase component $\chi'_{ac}$, which shifts to slightly higher temperatures with increasing frequency; the out-of-phase component $\chi''_{ac}$ scales with the driving frequency $f$, but exhibits no distinguishable feature at $T_{irr}$. This typical behaviour for a spin glass indicates that for $T < T_{irr}$ the magnetic moments respond on many different time scales, while they are acting as free spins for $T > T_{irr}$. For the sample with $x = 0.45$, however, $\chi'_{ac}$ is roughly temperature independent up to $T_{irr}$, where a kink in $\chi'_{ac}$ develops which is approximately frequency and temperature independent; $\chi''_{ac}$ scales with $f$ for $T > T_{irr}$, but the 10 Hz curve shows a drastic deviation from the other two for $T < T_{irr}$. This behaviour

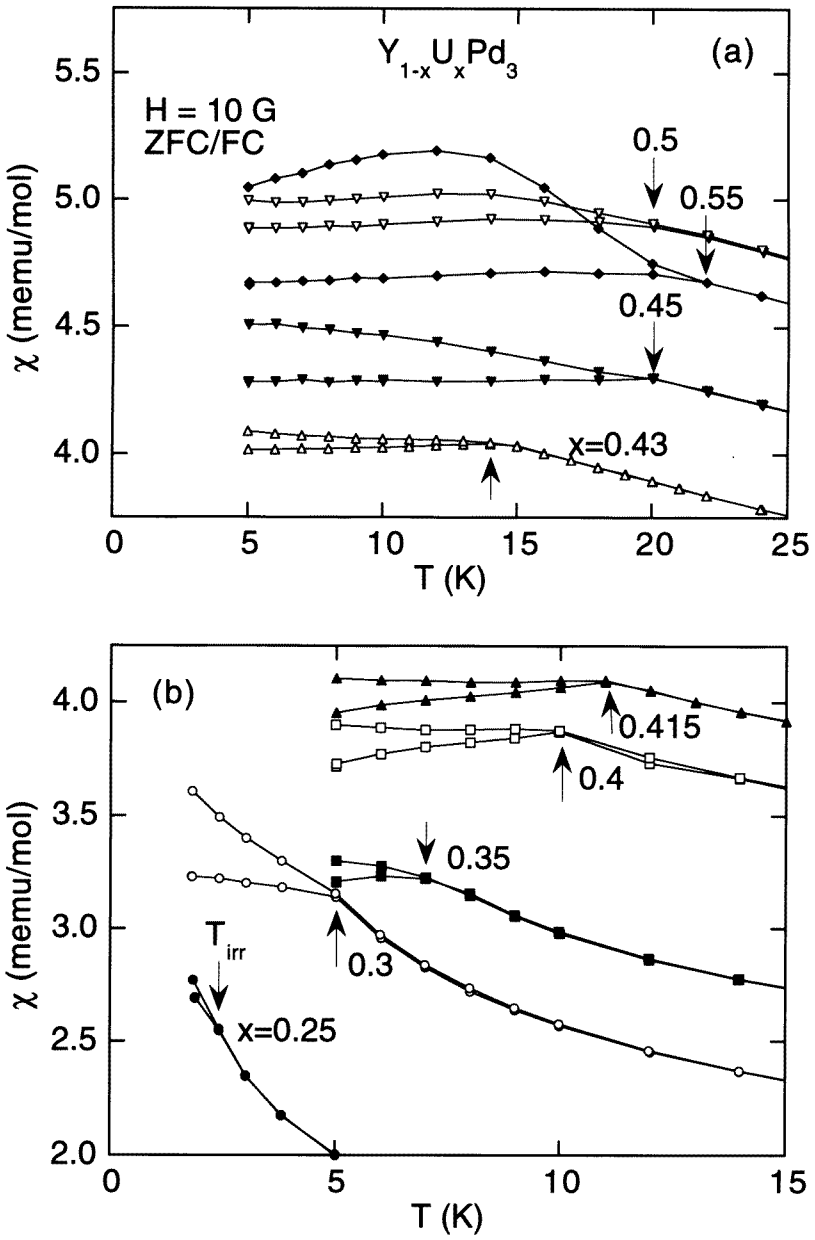


**Figure 5.** The magnetic susceptibility of $Y_{1-x}U_xPd_3$ under ZFC and FC conditions with an applied magnetic field of 10 G. For each measurement, the upper curve corresponds to FC, while the lower curve is for ZFC. (a) $0.43 \leqslant x \leqslant 0.55$; (b) $0.25 \leqslant x \leqslant 0.415$.

for $x = 0.45$ is typical of long-range antiferromagnetism, in that the response times are larger than those seen in a spin glass, and the features in $\chi_{ac}$ are sharper.

Shown in figure 7 are the results of magnetic relaxation experiments performed on samples with (a) $x = 0.4$ and (b) $x = 0.45$. In these experiments, the sample was heated

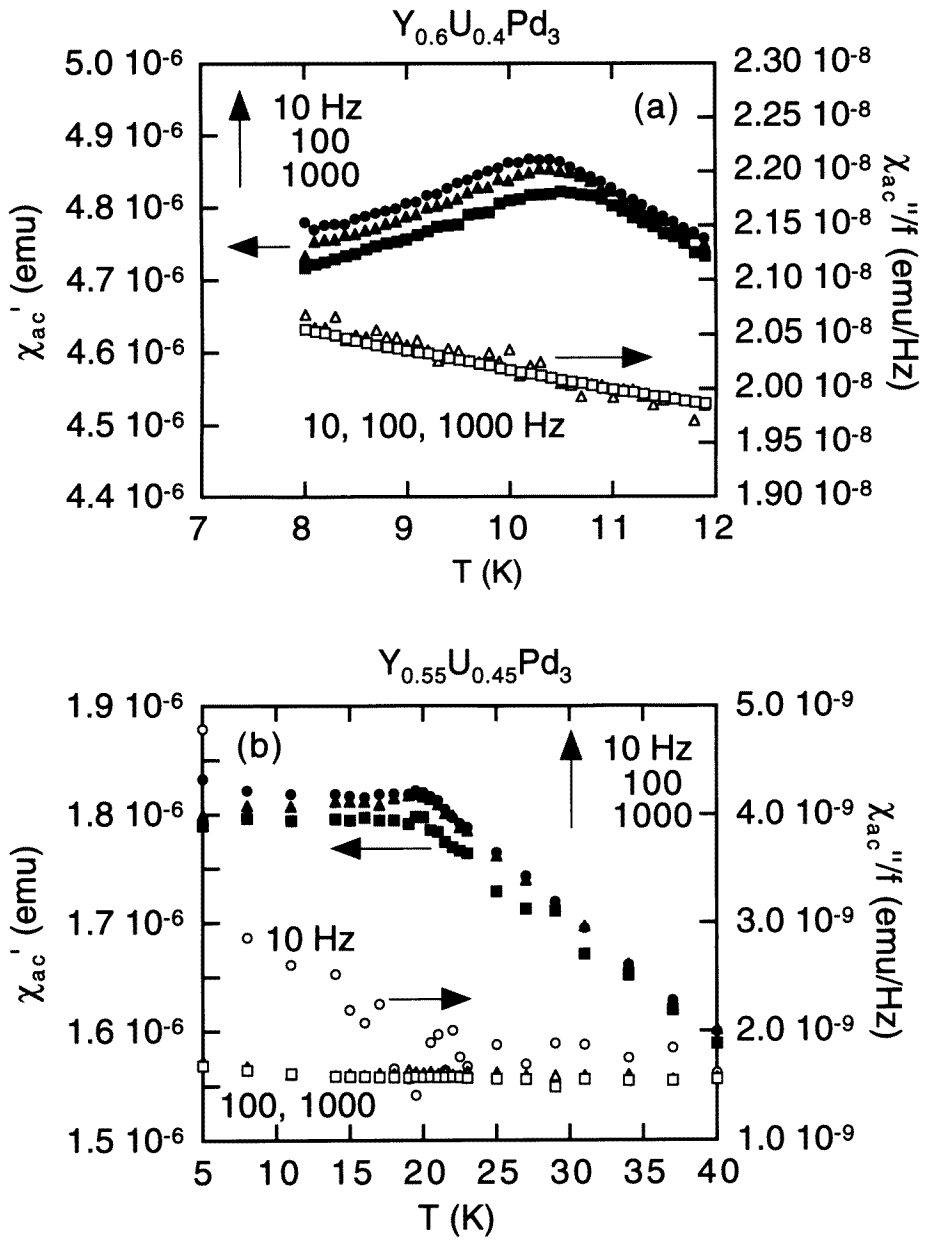


**Figure 6.** In phase ($\chi'_{ac}$) and out of phase ($\chi''_{ac}$) components of the ac susceptibility $\chi_{ac}$ of $Y_{1-x}U_xPd_3$ ($x = 0.4$ and 0.45) versus temperature $T$ at frequencies of 10, 100, and 1000 Hz. $\chi''_{ac}$ is scaled by the driving frequency $f$. (a) $Y_{0.6}U_{0.4}Pd_3$; (b) $Y_{0.55}U_{0.45}Pd_3$.

to a temperature well above its $T_{irr}$ (usually 40 K), where the sample was centred in the magnetometer in a 10 G field. The field was then set to zero, the sample was cooled to below its $T_{irr}$, the field was set again to 10 G, and magnetization was measured as a function of time. As shown in figure 7(a), the sample with $x = 0.4$ relaxed to approximately 40%

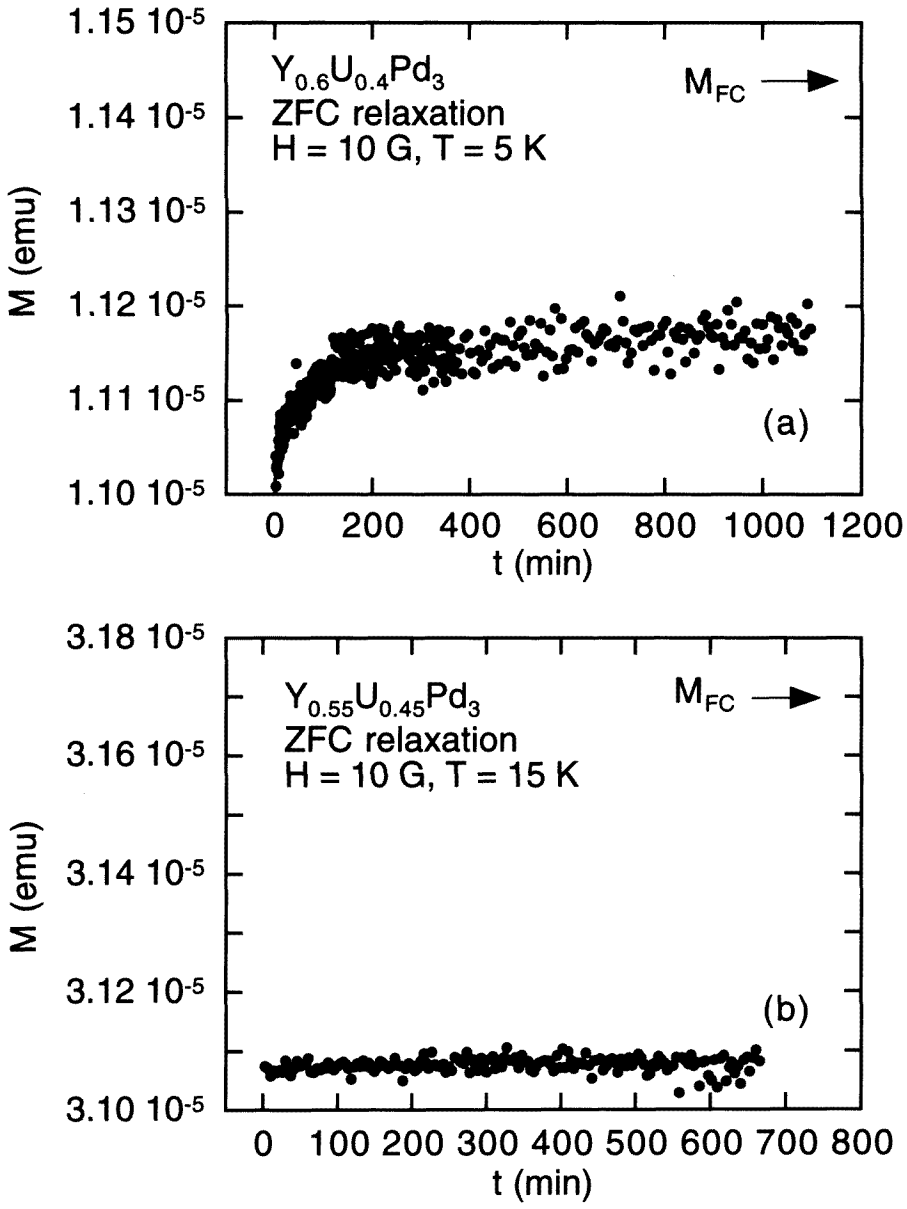


**Figure 7.** ZFC relaxation magnetization $M$ as a function of time, at an applied field of 10 G, of $Y_{1-x}U_xPd_3$ for (a) $x = 0.4$ and (b) $x = 0.45$. $M_{FC}$ represents the field cooled value of the magnetization at the measurement temperature.

of its FC value after approximately 20 h. In contrast, the magnetization of a sample with $x = 0.45$, shown in figure 7(b), showed no significant relaxation even after 10 h. Other measurements on samples in the proposed spin glass regime showed relaxation of the order of 10 h, while those in the AFM regime of the phase diagram exhibited no relaxation over the time scale of 1 d. Thus, the relaxation measurements are able to distinguish between

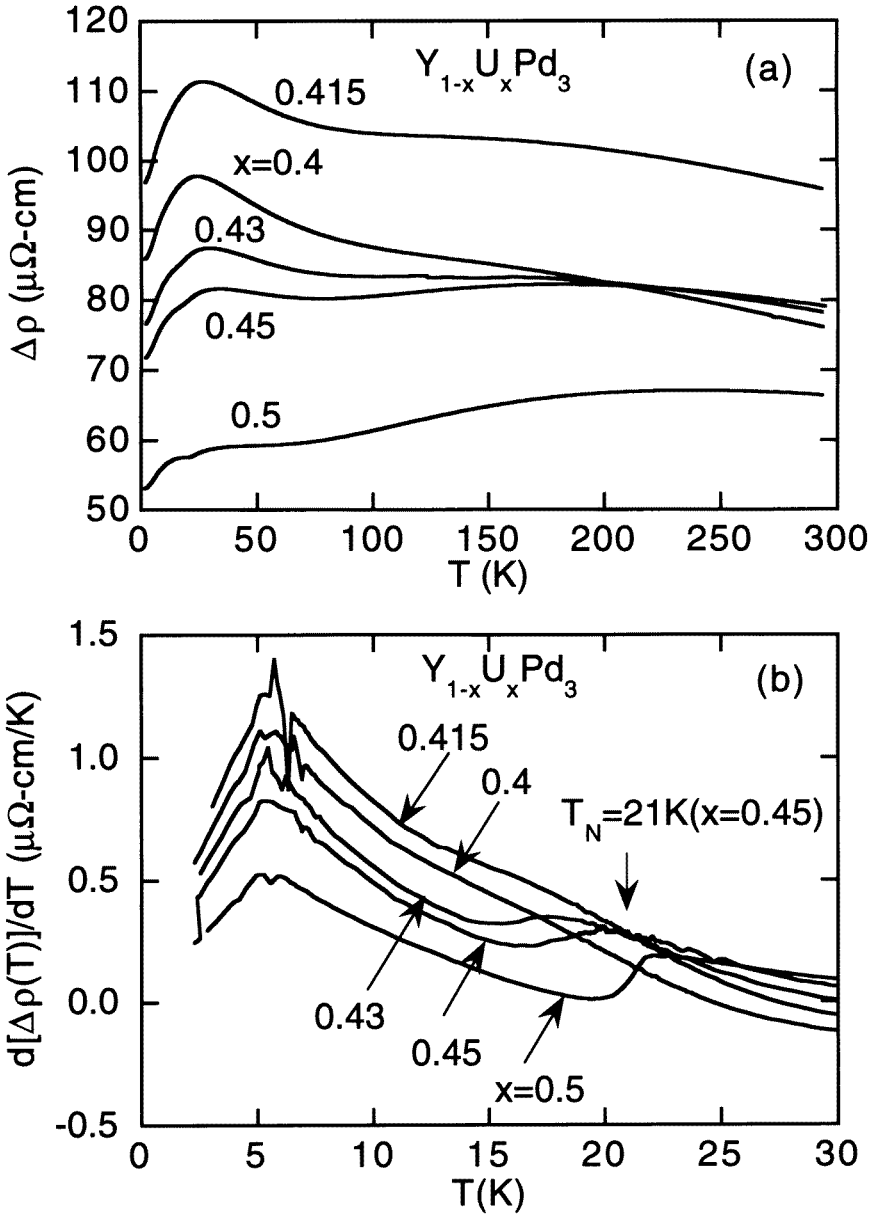


**Figure 8.** (a) Electrical resistivity $\Delta\rho(T)$ versus temperature $T$ of $Y_{1-x}U_xPd_3$ for $x = 0.4$, 0.415, 0.43, 0.45, and 0.5. (b) Derivative of the electrical resistivity with respect to temperature $T$, $d[\Delta\rho(T)]/dT$, versus $T$ for the same samples.

short-range spin glass and long-range AFM ordering and establish the boundary ($x \approx 0.42$) between these two types of magnetic order.

The relaxation data for $x = 0.4$ seem to approximately follow a stretched exponential behaviour, which is typical for spin glasses; however, a consistent quantitative analysis was not possible with this method. Each measurement with the magnetometer takes of the

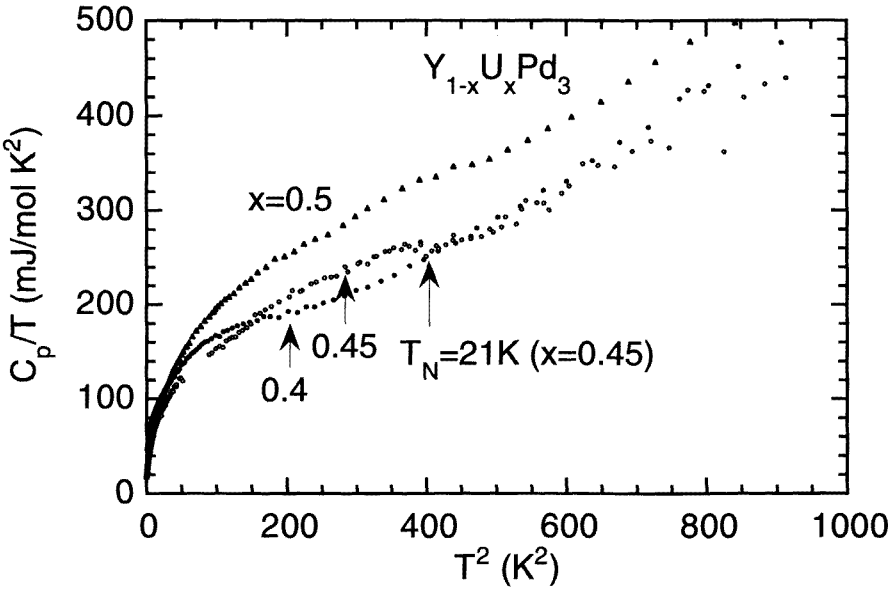


**Figure 9.** Specific heat $C_p$ divided by temperature $T$, $C_p/T$, versus $T^2$ of $Y_{1-x}U_xPd_3$ for $x = 0.4$, 0.45, and 0.5.

order of 1 min, which produces large errors in time, especially when the time is small. In addition, the magnetometer uses a stepper motor to physically move the sample through four second-derivative pickup coils with a scan length of 3 cm to perform the measurement. Some preliminary data taken using a new SQUID magnetometer with a reciprocating sample option, which reduces the measurement time to a few seconds and the scan length to 4 mm, produced curves which could be described by a stretched exponential law much better, and had much less scatter in the data. This may indicate that the long scan length of 3 cm used in some commercial SQUID magnetometers is subjecting the sample to an inhomogeneous magnetic field during the measurement, which could have a significant effect on the magnetization of samples that exhibit hysteretic magnetic behaviour such as spin glasses. Measurements are in progress to investigate this hypothesis further, and to obtain better relaxation data across the phase diagram.

The electrical resistivity $\Delta\rho(T)$ as a function of temperature for several samples near the spin glass–AFM transition is shown in figure 8(a), where $\Delta\rho(T) = \rho(T) - \rho(T, x = 0)$. For $x = 0.4$ and 0.415, $\Delta\rho(T)$ increases with decreasing temperature down to approximately 35 K, due to the magnetic impurity scattering, followed by a broad maximum at approximately 30 K, consistent with spin glass freezing. Samples with $x = 0.43$, 0.45, and 0.5 show similar behaviour, but in addition exhibit a rather sharp feature at lower temperatures. This feature is highlighted in figure 8(b), in which the derivative of the resistivity with respect to temperature, $\mathrm{d}[\Delta\rho(T)]/\mathrm{d}T$, is plotted versus temperature. Here, one sees a rather sharp feature in the AFM samples which approximately corresponds to $T_{irr}$; however, only a broad maximum can be seen in the spin glass samples.

Finally, the specific heat is plotted as $\Delta C_p(T)/T$ versus $T^2$ in figure 9. For the sample with $x = 0.4$, the $\Delta C_p(T)/T$ data display a rather broad maximum, presumably due to spin glass order, while for the sample with $x = 0.45$, the $\Delta C_p(T)/T$ data exhibit a rather

sharp feature which coincides well with $T_N$ as measured by neutron scattering. The feature near $T_N$ is surprisingly small for long-range AFM order, and is apparently even smaller for $x = 0.5$.

## 4. Summary

The electrical resistivity of the $Y_{1-x}U_xPd_3$ system approaches a constant value linearly with decreasing temperature for $x = 0.05$, 0.1, and 0.15, in agreement with the behaviour observed for the $x = 0.2$ compound. However, there is a small deviation from this behaviour at low temperatures, which is in need of further characterization. In addition, the intrinsic magnetic susceptibility of $Y_{0.9}U_{0.1}Pd_3$ approximately follows a square root temperature dependence, like that for $x = 0.2$, although it appears to level off below $\sim$5 K. These low-temperature departures of $\rho(T)$ and $\chi(T)$ from $T$ and $T^{1/2}$ dependences, respectively, could represent a crossover to Fermi liquid behaviour at low temperatures for uranium concentrations $x < 0.2$, but more experiments at lower temperatures are needed to resolve this issue.

dc and ac magnetic susceptibility, magnetic relaxation, electrical resistivity, and specific heat measurements have been performed on several samples in the magnetic ordering region of the $T$–$x$ phase diagram of $Y_{1-x}U_xPd_3$. These measurements have allowed us to conclusively determine that the boundary between short-range spin glass freezing and long-range AFM ordering lies approximately at $x = 0.42$ in this system. These results provide important information for any model that would attempt to ascribe the non-Fermi-liquid behaviour observed in this system for $x < 0.25$ to fluctuations of an order parameter above a second-order magnetic phase transition at $T = 0$.

## Acknowledgments

We would like to thank S Spagna and R Sager at Quantum Design Inc. for use of their prototype RSO SQUID magnetometer, and for many helpful discussions. This research was supported by the National Science Foundation under grant No DMR-94-08835.

## References

[1] Seaman C L, Maple M B, Lee B W, Ghamaty S, Torikachvili M S, Kang J-S, Liu L Z, Allen J W and Cox D L 1991 *Phys. Rev. Lett.* **67** 2882; 1992 *J. Alloys Compounds* **181** 327
[2] Andraka B and Tsvelik A M 1991 *Phys. Rev. Lett.* **67** 2886
[3] Kang J-S, Allen J W, Maple M B, Torikachvili M S, Ellis W P, Pate B B, Shen Z-X, Yeh J J and Lindau I 1989 *Phys. Rev.* B **39** 13 529
[4] Maple M B, Seaman C L, Gajewski D A, Dalichaouch Y, Barbetta V B, de Andrade M C, Mook H A, Lukefahr H G, Bernal O O and McLaughlin D E 1994 *J. Low Temp. Phys.* **95** 223
[5] Mook H A, Seaman C L, Maple M B, Lopez de la Torre M A, Cox D L and Makivic M 1993 *Physica* B **186–199** 341
[6] Dai P, Mook H A, Seaman C L, Maple M B and Koster J P 1995 *Phys. Rev. Lett.* **75** 1202
[7] Cox D L 1993 *Physica* B **186–188** 312
[8] McCarten J, Brown S E, Seaman C L and Maple M B 1994 *Phys. Rev.* B **49** 6400
[9] Aoki Y, Terayama K, Sato H, Maeda K and Onuki Y 1995 *Physica* B **206 & 207** 451
[10] von Löhneysen H, Pietrus T, Portisch G, Schlager H G, Schröder A, Sieck M and Trappmann T 1994 *Phys. Rev. Lett.* **72** 3262
[11] Mydosh J A 1993 *Spin Glasses* (Cambridge: Cambridge University Press)
[12] Lopez de la Torre M A 1996 *J. Appl. Phys.* **79** 6364

[13] Wu W D, Keren A, Le L P, Luke G M, Sternlieb B J, Uemura Y J, Seaman C L, Dalichaouch Y and Maple M B 1994 *Phys. Rev. Lett.* **72** 3722
[14] Maple M B, Dickey R P, Herrmann J, de Andrade M C, Freeman E J, Gajewski D A and Chau R 1996 *J. Phys.: Condens. Matter* **8** 9773–91
[15] Lukefahr H G, Bernal O O, MacLaughlin D E, Seaman C L, Maple M B and Andraka B 1995 *Phys. Rev.* B **52** 3038
[16] Gardner W E, Penfold J, Smith T F and Harris I R 1972 *J. Phys. F: Met. Phys.* **2** 133